

Study of Antimicrobial Activity of ZnO Nanoparticles Dopped Natural Hydroxyapatites

Dirgha Raj Karki¹, Sushant Bhujel¹, Kshama Parajuli^{1*}, Ramesh Raj Pant²,
Motee Lal Sharma^{1*}

¹Central Department of Chemistry, Institute of Science and Technology, Tribhuvan University, Kirtipur, Kathmandu, Nepal

²Central Department of Environmental Science, Institute of Science and Technology, Tribhuvan University, Kirtipur, Kathmandu, Nepal

Corresponding Email: ml.sharma@cdc.tu.edu.np, kshamaparajuli@yahoo.com

Submitted 6/29/2023, revised: 09/09/2023. Accepted 10/29/2023

Abstract

Bone replacements and repairs often encounter infections from diverse microbes, necessitating costly and painful secondary surgeries and treatments. Developing antimicrobial bone implants is crucial to mitigate these complications and enhance regeneration. Moreover, the biological synthesis of hydroxyapatite $\text{Ca}_{10}(\text{PO}_4)_6(\text{OH})_2$, a primary component of human bone, presents advantages over chemically synthesized alternatives due to lower impurity and cost. This study focuses on synthesizing hydroxyapatite powders from buffalo and goat femoral bones, with the incorporation of ZnO nanoparticles. Analyzed via XRD and FTIR, the prepared powder exhibited potent antimicrobial properties against various bacterial strains. Specifically, the hydroxyapatite powder doped with ZnO nanoparticles displayed superior antimicrobial activity. Consequently, this synthesized material holds significant promise for applications in bone tissue engineering and related fields.

Keywords: Bonewaste, ZnO nanoparticles, Hydroxyapatite, Antimicrobial activity, Bone tissue engineering

Introduction

Biomaterials play a critical role in repairing and replacing damaged living tissues, functioning in tandem with the body's natural systems. Among these biomaterials are inorganic substances synthesized through heating and cooling processes, known as bioceramics [1]. Bioceramics, whether crystalline, half-crystalline, or amorphous, serve various purposes such as tissue replacements and coatings. They

facilitate the body's restructuring of damaged tissues, enhancing biocompatibility and storage capabilities [2,3]. Additionally, they offer temporary solutions for damaged body parts.

Calcium orthophosphate-based bioceramics serve a crucial role in alleviating pain and restoring damaged calcified body tissues due to their remarkable surface bioactivity [4,5]. These bioceramics encompass various types of calcium orthophosphates, each

characterized by distinct Ca/P ratios ranging from 0.5 to 2. A lower Ca/P ratio results in a more acidic and water-soluble calcium orthophosphate [6]. Hydroxyapatite (HA or HAp), with a Ca/P ratio of 1.67, stands as the most stable and least soluble apatite. Hydroxyapatite powder can be synthesized through two primary methods: chemical synthesis and natural resources. However, the conventional chemical synthesis route often presents drawbacks such as impurity incorporation and high costs [7,8]. In contrast, natural resource-based methods utilize diverse sources like mammalian bones (e.g., bovine, goat, camel), shell sources (e.g., eggshell, seashell), and marine or aquatic sources (e.g., fish bones, fish scales) to prepare natural HAp. The stable hexagonal structure of hydroxyapatite (Figure 1) with specific lattice constants is suggested as $a=b= 0.937 \text{ nm}$, $c= 0.688 \text{ nm}$, $\alpha=\beta= 90^\circ$ and $\gamma= 120^\circ$ [9]:

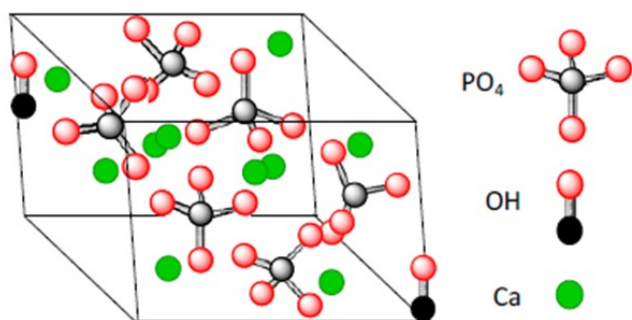


Figure 1: Structure of HAp crystal

Daily in Nepal, numerous cattle and buffalo bones are discarded as waste following meat processing, contributing significantly to environmental pollution. However, these discarded bones hold potential for the production of natural hydroxyapatite (HAp). Natural resource-derived HAp exhibits enhanced metabolic activity and dynamic response, elevating its widespread application [10], thereby garnering increased interest [11,12]. Despite its superior ability to bond with human hard tissues naturally [13,14], natural HAp possesses mediocre mechanical properties, including high brittleness, limited fracture toughness, low antimicrobial activity, and slow

solubility rates, restricting its application. To address these limitations, the enhancement of natural HAp properties through chemical doping and composite formation stands as a viable solution. These techniques influence the lattice parameters of HAp crystals, amplifying crystallinity and functionality [15]. Notably, the incorporation of ZnO nanoparticles (ZnO-NPs) uniformly dispersed within the HAp crystal structure enables various metal ions to occupy void areas [16]. The introduction of zinc alters the lattice parameter, reduces crystallinity, and affects the concentration of zinc, thereby influencing mechanical behavior. The distinctive mechanical behaviors observed in HAp with zinc doping arise from the differing sizes of Zn and Ca ions and their dissimilar melting temperatures. This interaction induces a phase change in HAp, augmenting fracture toughness [17].

Additionally, it is proposed that combining HAp with zinc and zinc oxide nanoparticles enhances osseointegration and biological responses, thus expanding the scope of biomedical applications [18]. Despite this potential, research in this domain remains scarce. Therefore, this study aimed to introduce ZnO nanoparticles (NPs) into natural HAp obtained from biowaste, with a focus on evaluating its antimicrobial properties against selected microorganisms.

Materials and Methods

Reagent-grade solvents and chemicals, including acetone, methanol, ethanol, zinc nitrate hexahydrate, dimethyl sulfoxide, sodium hydroxide, among others, were sourced from Loba Chemicals. Nutrient agar and nutrient broth were acquired from HiMedia Laboratories India. Distilled water served as the solvent throughout the experiments. All procedures were conducted at the Central Department of Chemistry, Institute of Science and Technology, Tribhuvan University, Kathmandu, Nepal.

Bacterial source: Five bacterial strains, specifically gram-negative bacteria (*Escherichia coli*-ATCC 88553, *Klebsiella pneumoniae*-ATCC 700603, and *Pseudomonas aeruginosa*-ATCC 27853) and gram-positive bacteria (*Staphylococcus aureus*-ATCC 43300 and *Bacillus subtilis*) were sourced from the Central Department of Microbiology, Institute of Science and Technology, Tribhuvan University, Kathmandu, Nepal.

Synthesis of HAp powders: Hydroxyapatite powder was derived from the pristine femoral sections of goat and buffalo bones using a straightforward calcination process at 850°C for 4 hours. The resulting powder sample underwent a 10-minute sonication process followed by filtration. The residue was subsequently dried at 60°C in a hot air oven, resulting in the designation of GHAp and BHAp for hydroxyapatite obtained from goat and buffalo bones, respectively [17].

Preparation of ZnO nanoparticles: ZnO nanoparticles were synthesized following the methodology outlined in the literature [19]. In summary, a 0.1 M solution of zinc nitrate hexahydrate ($Zn(NO_3)_6 \cdot 6H_2O$) was prepared, and a 0.1 M NaOH solution was added dropwise over 30 minutes while continuously stirring. The mixture was then left overnight for the supernatant liquid. Subsequently, the liquid was centrifuged for 10 minutes at 8000 rpm. The resulting precipitate was washed with water and ethanol before being dried in a hot air oven.

Doping of ZnO NPs to hydroxyapatite powders: A suspension of ZnO and HAp powders was prepared and placed in a rotary shaker for 48 hours. Afterward, the suspension underwent centrifugation for 10 minutes at 8000 rpm. The resulting supernatant liquid was separated, and the remaining powders were dried at 60°C in a hot air oven [20].

Characterizations: The synthesized HAp, ZnO NPs, and ZnO NPs doped hydroxyapatite powders underwent analysis via X-ray diffractometry at the Nepal Academy of Science and Technology (NAST), Khumaltar, Lalitpur, Nepal, conducted at room temperature within a 2θ angle range of 10-80. Additionally, Fourier Transform Infrared Spectroscopy analysis was performed on the prepared powders in ATR mode, spanning the range of 400-4000 cm^{-1} , at the Central Department of Chemistry, Institute of Science and Technology, Tribhuvan University, Nepal.

Antimicrobial study: The sample solutions for antimicrobial screening were prepared in 50% DMSO at a concentration of 50 mg/mL. These solutions underwent the antimicrobial test using the well disc diffusion method against the aforementioned five bacterial strains. Initially, fresh bacterial cultures were incubated for a full 24 hours at 37°C to ensure complete growth. Blank paper discs of 6 mm diameter were prepared using Whatman number 1 filter paper, sterilized, and subsequently loaded with the sample solutions. The revived pathogens were gently swabbed onto sterile Muller Hinton Agar (MHA) media specifically prepared for the antimicrobial test. The loaded paper discs, containing concentrations of 20 μL per disc, were placed onto the agar. Neomycin served as the positive control, while DMSO acted as the negative control throughout the process. Following this setup, the Petri dishes were incubated at 37°C for 24 hours to observe the zone of inhibition, indicating the effectiveness of the sample solutions against the various bacterial strains.

Results and discussion

XRD study

XRD serves as a versatile non-destructive analytical technique utilized for the identification and quantitative determination of crystalline forms [21]. Additionally, it plays a pivotal role in evaluating the

phase purity of synthesized samples [22]. Figure 2(a) shows the X-ray diffraction pattern of the isolated material from waste bone powder and as can be seen from the figure that there were distinct peaks observed at 2θ angle of 31.83° , 32.86° , 34.04° , 39.74° , and 46.66° assigned to 211, 300, 202, 310, and 222 miller planes confirming the crystallinity and as well as phase purity of the isolated HAp and no other other mineral phases were identified [11]. Further, in Figure 2(b), X-ray diffraction of the prepared ZnO NPs where intense sharp crystalline peaks were observed confirming the crystalline nature and phase purity of the synthesized nanopowder. Crystalline peaks were observed at 2θ angles of 31.72° , 34.36° , 36.19° , 47.50° , 56.56° , and 62.77° assigned to 100, 002, 101, 102, 110, and 103 miller planes. All the peaks seen could be indexed as the zinc oxide wurtzite structure (JCPDS Data Card No: 36-1451) [23]. Mainly, zinc oxide possessed two main types of crystals, hexagonal wurtzite, and cubic zinc blende. The wurtzite is most stable at ambient conditions and thus most common. It also confirmed the synthesized nano powder was free of impurities as it does not contain any characteristics of XRD peaks other than zinc oxide peaks. Similarly, in Figure 2(c), XRD of the ZnO NPs doped HAp is given and it showed intense and sharp crystalline peaks at the 2θ angle of 31.66° , 34.34° , 36.14° , 47.36° , 56.46° , and 62.78° . The analysis came with the agreement as done by [24]. Further particle size of ZnO NPs doped HAp was found to be 5.71 nm as calculated with the help of the Debye-Scherrer formula (Eq-1) [25].

$$D = k\lambda/\beta\cos\theta \dots\dots\dots (Eq-1)$$

Where D = Crystallite size, k = proportionality constant (0.9), λ = X-ray wavelength (1.54178 \AA), β = FWHM (full width at half maxima) of XRD peaks, θ = Bragg's angle

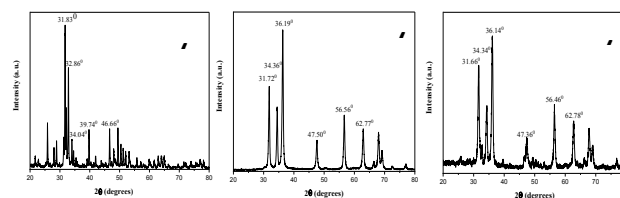


Figure 2. XRD of (a) HAp powder (b) ZnO NPs (c) ZnO NPs doped HAp powder

FTIR study

FTIR study hint the possible functional groups present in the prepared sample. In Figure 3(a), FTIR spectrum of the synthesized hydroxyapatite from waste buffalo bone powder calcined at 850°C temperature. The hydroxyapatite represents a naturally occurring mineral form of calcium apatite, characterized by the chemical formula $\text{Ca}_5(\text{PO}_4)_3(\text{OH})$. It is often denoted as $\text{Ca}_{10}(\text{PO}_4)_6(\text{OH})_2$ to signify the crystal unit cell's two entities, it stands as the hydroxyl endmember within the diverse apatite group. Figure 3(a) illustrated the presence of phosphate group (PO_4^{3-}), carbonate group (CO_3^{2-}), and hydroxyl groups (OH^-) in the prepared sample. The bands that appeared in the range of $962\text{--}1105 \text{ cm}^{-1}$ indicated the phosphate (PO_4^{3-}) groups stretching while the small band appeared in the range 1400 cm^{-1} assigned to the carbonate (CO_3^{2-}) group. The broader band appeared in the range of $2500\text{--}3700 \text{ cm}^{-1}$ corresponding to absorbed water. Also, the band located at approximately 3350 cm^{-1} was due to the stretching of the hydroxyl group. The absorption band appeared at the 629 cm^{-1} assigned to the OH vibrational mode. At 561 cm^{-1} is due to the bending of phosphate groups [19,26]. Likewise the FTIR spectrum of the synthesized ZnO NPs is shown in the Figure 3(b). The Zn-O stretching at the wavelength of 520 cm^{-1} while bending at 448 cm^{-1} appeared confirming the formation of ZnO nanopowder [21]. The weak peak at wavelength 1633 cm^{-1} showed the presence of the carbonyl group and the wide peak at wavelength 3300 cm^{-1} showed the presence of the hydroxyl group probable due to moisture present in the sample. Similarly Figure 3(c), represents FTIR spectrum of the

ZnO doped HAp where a weak and broader band at 3400 cm^{-1} indicated the stretching of the hydroxyl group and the peaks appeared at 473 cm^{-1} and 596 cm^{-1} was related to the presence of stretching Zn-O group and this band seem to be overlapped with the bending vibrations of the phosphate group. The appearance of a band at 1466 cm^{-1} assigned to the carbonyl group C=O and a weak band at 3400 cm^{-1} indicated the stretching of the hydroxyl group [24].

nanoparticles doped hydroxyapatite powder showed the zone of inhibition against the most of all bacterial strains investigated in this study. Further, from the observed results, it can be deduced that, the ZnO nanoparticles separately and their doped version with bone-based hydroxyapatite powders are the potential material for antimicrobial activity and can be used in the repair and replacement of bone damages without worrying about the post-treatment surgeries.

Table 1. Observed Zone of Inhibition of the prepared

Bacterial strains	Observed zone of inhibition (mm)				
	ZnO	ZnO+G	ZnO+B	PC	NC
<i>Escherichia coli</i>	12	11	14	20	-
<i>Klebsiella pneumonia</i>	11	10	13	18	-
<i>Pseudomonas aeruginosa</i>	10	9	12	16	-
<i>Staphylococcus aureus</i>	12	12	15	15	-
<i>Bacillus subtilis</i>	12	10	14	26	-

samples against various bacterial strains

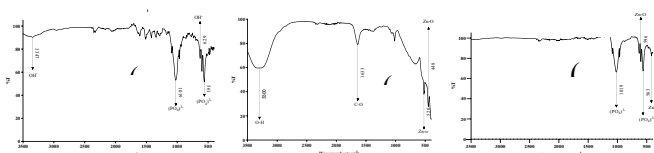


Figure 3. FTIR spectrum of (a) buffalo based HAp powder (b) ZnO NPs (c) ZnO NPs doped buffalo-based HAp powder

Antimicrobial activity

The antimicrobial activity of the prepared samples were screened for the antimicrobial test against the five bacterial strains i.e., gram-negative bacteria *Escherichia coli*, *Klebsiella pneumoniae*, *Pseudomonas aeruginosa*, and gram-positive bacteria namely *Staphylococcus aureus* and *Bacillus subtilis*. In Figure 4 photograph of the antimicrobial study is given and the observed the zone of inhibition was summarized in the Table 1. As seen from the Table 1, both as prepared ZnO nanoparticles and ZnO

Where ZnO+G= ZnO NPs doped goat bone based HAp, ZnO +B= ZnO NPs doped goat bone based HAp, PC = positive control and NC = positive control



Figure 4. Photograph of in vitro antibacterial screening of synthesized powders against *Klebsiella pneumoniae*

Conclusions

We synthesized white, water-insoluble hydroxyapatite using natural resources—specifically, femoral waste bones from goats and buffaloes. Employing the chemical precipitation method with zinc nitrate hexahydrate and sodium hydroxide as precursors, we synthesized white zinc oxide nanopowder. Subsequently, the synthesized ZnO nanoparticles were incorporated into isolated HAp obtained from both biological sources. The XRD analysis confirmed the crystalline nature and phase purity of the synthesized nanopowder, evident from intense, sharp crystalline peaks. Furthermore, the FTIR analysis verified the presence of essential functional groups such as PO_4^{3-} and OH^- in the isolated hydroxyapatite powders. The FTIR analysis of ZnO NPs revealed a peak around 447 cm^{-1} , confirming the presence of Zn-O vibrations. Additionally, when examining the zinc oxide nanoparticles doped hydroxyapatite powders, the FTIR analysis indicated similar peaks to the original HAp

powders, affirming the presence of ZnO doped into HAp. Notably, characteristic peaks around 447 cm^{-1} further confirmed the incorporation of ZnO within the HAp structure. The antimicrobial screening of the prepared samples using the disc diffusion method upon the two different types of five bacterial strains i.e., gram-negative bacterial strains (*Escherichia coli*, *Klebsiella pneumoniae*, and *Pseudomonas aeruginosa*) and gram-positive bacterial strains (*Staphylococcus aureus* and *Bacillus subtilis*) confirming the importance of their potential use for the recovery and repairment of the damaged bone and bone tissues in the biomedical field. Finally, the synthesis of hydroxyapatite from waste bones, augmented with ZnO nanoparticles, shows promise for biomedical applications in bone repair; further exploration of its efficacy and safety in clinical settings is recommended.

References

- [1] S. V. Dorozhkin, Calcium orthophosphate-based bioceramics, *Materials (Basel)*, 2013,**6**, 3840–3942. <https://doi.org/10.3390/ma6093840>.
- [2] R. Heimann, Materials science of crystalline bioceramics: a review of basic properties and applications, *Chiang Mai Univ. J.*, 2002,**1**, 23–46.
- [3] L.L. Hench, D.E. Day, W. Höland, V.M. Rheinberger, Glass and medicine, *Int. J. Appl. Glas. Sci.*, 2010,**1**, 104–117. <https://doi.org/10.1111/j.2041-1294.2010.00001.x>.
- [4] L.L. Hench, Bioceramics, *J. Am. Ceram. Soc.*, 1998,**81**, 1705–1728. <https://doi.org/10.1111/j.1151-2916.1998.tb02540.x>.
- [5] E.Y. Kawachi, C.A. Bertran, R.R. Dos Reis, O.L. Alves, Biocerâmicas: Tendências e perspectivas de uma área interdisciplinar, *Quim. Nova.*, 2000,**23**, 518–522. <https://doi.org/10.1590/S0100-40422000000400015>.
- [6] L. Wang, N.H. George, Calcium orthophosphates: Crystallization and dissolution, *Chem. Rev.*, 2008,**108**, 4628–4669.
- [7] N.I. Agbeboh, I.O. Oladele, O.O. Daramola, A.A. Adediran, O.O. Olasukanmi, M.O. Tanimola, <https://www.nepjol.info/index.php/JNCS>

- Environmentally sustainable processes for the synthesis of hydroxyapatite, *Heliyon*, 2020, **6(4)**, e03765. <https://doi.org/10.1016/j.heliyon.2020.e03765>.
- [8] W.J. Shih, M.C. Wang, M.H. Hon, Morphology and crystallinity of the nanosized hydroxyapatite synthesized by hydrolysis using cetyltrimethylammonium bromide (CTAB) as a surfactant, *J. Cryst. Growth.*, 2005, **275**, 2339–2344. <https://doi.org/10.1016/j.jcrysgro.2004.11.330>.
- [9] R. Sawittree, K. Pitoon, Panthong W, Synthesis of Hydroxyapatite from Oyster Shell via Precipitation. *Energy Procedia* 56 (2014) 112 – 117. <https://doi.org/10.1016/J.EGYPRO.2014.07.138>
- [10] M. Akram, R. Ahmed, I. Shakir, W.A.W. Ibrahim, R. Hussain, Extracting hydroxyapatite and its precursors from natural resources, *J. Mater. Sci.*, 2014, **49**, 1461–1475. <https://doi.org/10.1007/s10853-013-7864-x>.
- [11] K. Parajuli, K.P.Malla, N.Panchen, G.C. Ganga, R. Adhikari, Isolation of antibacterial nano-hydroxyapatite biomaterial from waste buffalo bone and its characterization, *Chem. Chem. Technol.*, 2022, **16(1)**, 133-141, <https://doi.org/10.23939/chcht16.01.133>.
- [12] F. Heidari, M. Razavi, M. Ghaedi, M. Forooghi, M. Tahriri, L. Tayebi, Investigation of mechanical properties of natural hydroxyapatite samples prepared by cold isostatic pressing method, *J. Alloys Compd.*, 2017, **693**, 1150–1156. <https://doi.org/10.1016/j.jallcom.2016.10.081>.
- [13] N.A. Zakharov, I.A. Polunina, K.E. Polunin, N.M. Rakitina, E.I. Kochetkova, N.P. Sokolova, V.T. Kalinnikov, Calcium hydroxyapatite for medical applications, *Inorg. Mater.*, 2004, **40**, 641–648. <https://doi.org/10.1023/B:INMA.0000032000.83171.9f>.
- [14] G. Daculsi, O. Laboux, O. Malard, P. Weiss, Current state of the art of biphasic calcium phosphate bioceramics, *J. Mater. Sci. Mater. Med.*, 2003, **14**, 195–200. <https://doi.org/10.1023/A:1022842404495>.
- [15] M. Šupová, Substituted hydroxyapatites for biomedical applications: A review, *Ceram. Int.*, 2015, **41**, 9203–9231. <https://doi.org/10.1016/j.ceramint.2015.03.316>.
- [16] Mamat B, Zhang N, Yan L, Luo J, Xie C, Wang Y, Ma C, Ye T. Stable ZnO-doped Hydroxyapatite Nanocoating for Anti-infection and Osteogenic on Titanium, *Colloids Colloids Surf. B.*, 2019. <https://doi.org/10.1016/j.colsurfb.2019.110731>
- [17] V. Saxena, A. Hasan, L.M. Pandey, Effect of Zn/ZnO integration with hydroxyapatite: a review, *Mater. Technol.*, 2018, **33**, 79–92. <https://doi.org/10.1080/10667857.2017.1377972>.
- [18] W. Khoo, F.M. Nor, H. Ardhyanta, D. Kurniawan, Preparation of natural hydroxyapatite from bovine femur bones using calcination at various temperatures, *Procedia Manuf.*, 2015, **2**, 196–201. <https://doi.org/10.1016/j.promfg.2015.07.034>.
- [19] A.J. Ahamed, P. Vijaya Kumar, Synthesis and characterization of ZnO nanoparticles by co-precipitation method at room temperature, *J. Chem. Pharm. Res.*, 2016, **8**, 624–628.

- [20] M. Swetha, K. Sahithi, A. Moorthi, N. Saranya, S. Saravanan, K. Ramasamy, N. Srinivasan, N. Selvamurugan, Synthesis, characterization, and antimicrobial activity of nano-hydroxyapatite-zinc for bone tissue engineering applications, *J. Nanosci. Nanotechnol.*, 2012, **12**, 167–172. <https://doi.org/10.1166/jnn.2012.5142>.
- [21] R. L. Manjunnath, K.V. Usharani, & Naik, D. , Synthesis and characterization of ZnO nanoparticles: A review *J. pharmacogn. phytochem.*, **8(3)**, 1095–1101.
- [22] M. Figueiredo, A. Fernando, G. Martins, J. Freitas, F. Judas, H. Figueiredo, Effect of the calcination temperature on the composition and microstructure of hydroxyapatite derived from human and animal bone, *Ceram. Int.*, 2010, **36**, 2383–2393.
- [23] G.B. Karki , K.Parajuli , S. Adhikari , S. P. Khatiwada , R. Adhikari, Facile synthesis of zinc carbonate and zinc oxide nanoparticles and their antimicrobial properties, *J. Nepal Biotechnol.Assoc.*, 2023, *4 (1)*, 37-43.
- [24] M. Safari Gezaz, S. Mohammadi Aref, M. Khatamian, Investigation of structural properties of hydroxyapatite/ zinc oxide nanocomposites; an alternative candidate for replacement in recovery of bones in load-tolerating areas, *Mater. Chem. Phys.* 226 (2019) 169–176. <https://doi.org/10.1016/j.matchemphys.2019.01.005>.
- [25] K. Parajuli, A.K., Sah, H. Paudyal, Green synthesis of magnetite nanoparticles using aqueous leaves extracts of *Azadirachta indica* and its application for the removal of As(V) from water, *Green .Sustain. Chem.*, 2020, **10(04)**, 117–132. <https://doi.org/10.4236/gsc.2020.104009>
- [26] V. Stanić, S., Dimitrijević, J. Antić-Stanković, M. Mitrić, B. Jokić, I.B. Plećaš, S. Raičević, Synthesis, characterization and antimicrobial activity of copper and zinc-doped hydroxyapatite nanopowders. *Appl. Surf. Sci.*, 2010, **256(20)**, 6083–6089. <https://doi.org/10.1016/j.apsusc.2010.03.124>.